16th World Conference on Earthquake, 16WCEE 2017

Santiago Chile, January 9th to 13th 2017

Paper N° 370 (Abstract ID)

Registration Code: S-E1450653951

Design of Grid-Wall Soil Improvement to Mitigate Soil Liquefaction Damage in Residential Areas

S. Tsukuni[(1)], I. Ishii[(2)], A. Uchida[(3)], M. Imai[(4)], T. Yamauchi[(5)] and K. Ota[(6)]

[(1)] *General Manager, Takenaka Civil Engineering & Construction Co.,Ltd.,tsukuni-s@takenaka-doboku.co.jp*
[(2)] *Deputy Mayer, Urayasu City, ishii.ichirou@city.urayasu.lg.jp*
[(1)] *Senior Chief Researcher, Research and Development Institute, uchida.akihiko@takenaka.co.jp*
[(1)] *Member, Takenaka Civil Engineering & Construction Co., Ltd., imai-m@takenaka-doboku.co.jp*
[(1)] *Manager, Maeda Corporation, yamauchi.tak@jcity.maeda.co.jp*
[(1)] *Member, Maeda Corporation, oota.kou@jcity.maeda.co.jp*

Abstract

In the land reclamation areas of Urayasu city, 8,700 small buildings such as residential houses suffered severe damage due to liquefaction during the 2011 Tohoku earthquake. This represents almost one third of all houses in Japan that suffered severe damage due to liquefaction. Following this event, Urayasu city adopted grid-wall soil improvements as countermeasures to mitigate liquefaction. Investigations and design processes are ongoing for 4,103 residential houses, and the construction stage started in January 2016 for 44 residential houses. For the conditions of simplified grid-wall soil improvement design, the spacing between the grid-walls is restricted within L/H = 0.8. L is the spacing between the grid-walls and H is the thickness of the liquefaction layer. However it is difficult to adopt L/H as a design guideline because the grid-wall soil improvement has to be applied under existing houses. The construction of grid-walls directly under houses is impossible. Consequently, the spacing between the grid-walls increases. It is suitable to use the settlement of a house as a design guideline for the conditions in Urayasu. The finite element method with a quasi-three-dimensional analysis model can be used to estimate the settlement of houses. However, there are no examples that have adopted the settlement as a design guideline in grid-wall soil improvement design. As such, dynamic centrifuge model tests were conducted to investigate the relationship between the settlement of houses and the grid-area. The design method and numerical analysis was verified through the experiments.

Keywords: liquefaction, grid-wall soil improvement, centrifuge model test, settlement

1. Introduction

In the 2011 Tohoku earthquake (Moment Magnitude M_w = 9.0) many buildings suffered severe damage from tsunami. Furthermore, many residential houses suffered severe damage due to liquefaction. Liquefaction damage occurred at the riverside of the Tone river and the Tokyo Bay area, which were far from the epicenter. The twenty six thousands nine hundreds fourteen buildings in Japan suffered from severe damage caused by liquefaction. Urayasu city is located in the Tokyo Bay area and is very small, covering an area of 17.3 km^2 (Fig. 1). However, 8,700 buildings in the city suffered from severe damage. This represents almost one third of all houses in Japan that suffered from severe damage caused by liquefaction (Fig. 1). In Urayasu, the peak ground acceleration was 0.160 g (Fig. 2), which is relatively small. However, the duration of the seismic waves (hereafter called the Urayasu Wave) was about 200 seconds. Liquefaction was easily caused by the Urayasu Wave due to its long duration. The damaged area in Urayasu was restricted to land reclamation areas that were constructed using hydraulic dredging from 1965 to 1980. The most severe damage occurred at the Nakamachi area (Phot.1). There were many residential houses in this area.

In 2011, the government planned a subsidy countermeasure project to mitigate liquefaction for residential houses and roads (Fig. 3). The Ministry of Land Infrastructure and Transport (MLIT) organized a committee consisting of people with the required background knowledge and experience.

The city government of Urayasu also organized a committee consisting of people with the required background knowledge and experience (hereafter called the Urayasu committee) on July 2011. To begin, the Urayasu committee researched the relationship between the damage due to liquefaction and the ground properties. In 2012, the Urayasu committee researched countermeasures to mitigate liquefaction using the groundwater level lowering method and grid-wall soil improvements. Land reclamation area at Urayasu consists of several stratums. The upper stratum is fill (F) constructed with dredge soil, and just below F is loose alluvium sand (A_s). Loose and thick cohesive soil (A_c) deposits are just below A_s. During a field trial using the groundwater level lowering method, disparate and large settlement of the ground surface was observed due to consolidation of inhomogeneous of F stratum and A_c stratum. Consequently, the city government of Urayasu adopted grid-wall soil improvements as a countermeasure to mitigate from liquefaction. Figure 4 and Phot 2 show the concept of grid-wall soil improvements. The improved soil walls surround the residential house's grid-form shape in plan view. Grid-walls are constructed using the deep cement mixing method and are composed of overlapping

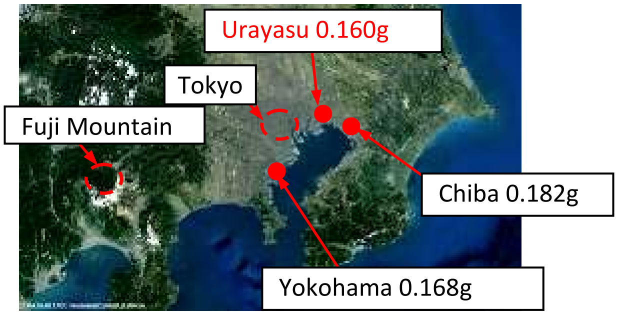

Fig. 1 Maximum horizontal acceleration due to the Tohoku earthquake in the Tokyo Bay area.

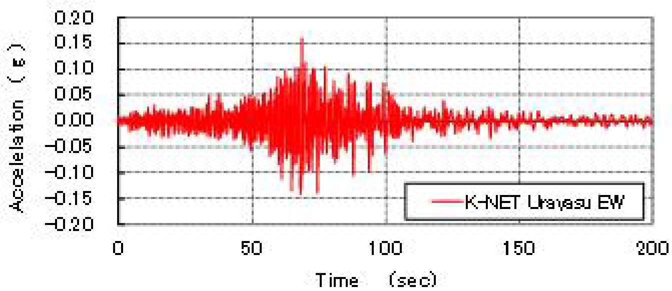

Fig. 2 Seismic wave observed in Urayasu (Urayasu Wave).

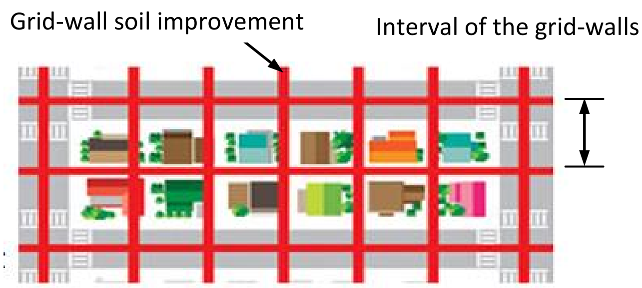

Fig. 3 A plan for grid-form deep mixing walls for roads and existing private houses.

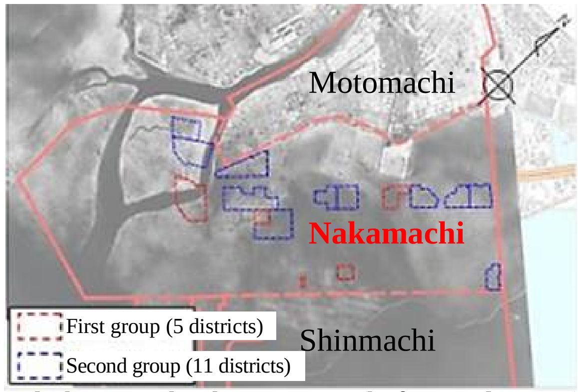

Phot. 1 Aerial photograph taken in 1948 (before reclamatin)

columns.

In 2014, residents of Urayasu City agreed to develop plans and cost estimates for using grid-wall soil improvements as a countermeasure. That plan was prepared for 4,103 residential houses in 16 districts. Geological surveys began in the same year. In 2015, design development for grid-wall soil improvements began. If the residents agree to the proposed plan and the estimated cost, the project will move to the construction stage. By March 2016, the plan and estimated cost have already been proposed to residents of 4,103 residential houses. The residents of 44 residential houses have agreed to move to the construction stage.

2. Design Policies

This chapter describes the design method for grid-wall soil improvements. Figure 5 explains the mechanism through which grid-wall soil improvement mitigates liquefaction. The left part of the diagram shows the outcome without countermeasures, in which large shearing deformation of the ground occurs during an earthquake. The right part of the diagram shows the outcome with the use of grid-wall soil improvement. Shear force concentrates on the grid-walls, thereby controlling the shear force generated in the ground.

Development of the grid-wall soil improvement technique was conducted from the late 1980s to the early 1990s. Under the conditions of simplified grid-wall soil improvement design, the spacing between the grid-walls is restricted within L/H = 0.8 according to experiments [1]. L is spacing between the grid-walls, and H is the thickness of the liquefaction layer. Figure 6 shows the relationship between L/H and the maximum excess pore pressure ratio obtained through experiments. If L/H is within 0.8, the maximum excess pore pressure ratio is within 0.5. Conversely, detailed grid-wall soil improvement design uses dynamic numerical analysis with the finite element method (FEM) [2]. The three-dimensional shape of grid-form walls are modeled using a two-dimensional analytical model. The shear stress generated in the ground is calculated from that produced by seismic waves. According to specifications [3], the calculated shear stress, the standard penetration test (SPT-) N value, and the fine fraction content of soils gives the liquefaction strength. Consequently, the safety factor against liquefaction (FL) can be calculated. During the 1995 Hyogo-ken Nanbu Earthquake, a hotel that adopted

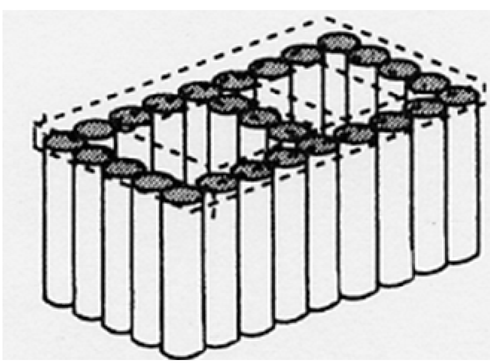

Fig.4 Grid-wall soil improvement.

Phot.2 Grid-wall soil improvement.

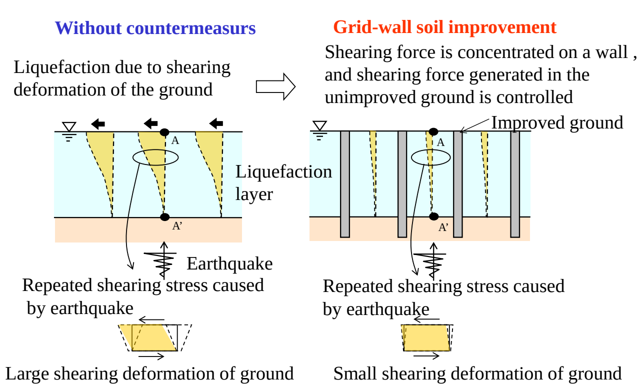

Fig.5 Mechanism through which liquefaction is mitigated with the use of grid-wall soil improvements.

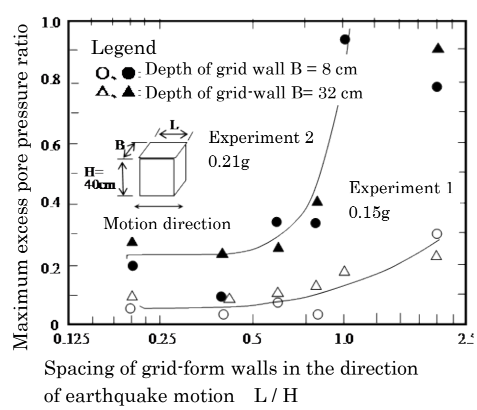

Fig.6 Relationship between the spacing of grid-walls and the maximum excess pore pressure ratio.

the detailed design method suffered from no damage due to liquefaction [2]. A theater in Urayasu also adopted the detailed design method, but had an *L*/*H* that exceeded 0.8. However, it also experienced no damage due to liquefaction [2]. Considering these result, the city government of Urayasu adopted grid-wall soil improvements as a countermeasure to mitigate liquefaction damage. Some problems still remain in application of grid-wall soil improvement to residential areas in Urayasu. The main damage caused by liquefaction to residential houses was house inclination (Phot. 3), because the bearing capacity of the ground decreased due to liquefaction. Now that residents are living in a damaged or a repaired house, the grid-walls will be built to roughly accommodate existing residential houses (it is not possible to construct the grid-walls directly beneath the houses). Therefore, a grid-wall is to be constructed between the spacing of residential houses. Due to such locations, the spacing between the grid-walls will be relatively wide. One solution could be to allow partial liquefaction, thus increasing the feasibility and reducing the cost of countermeasures. Unfortunately, there are no quantifiable data on the relationship between the spacing of grid-walls and ground settlement. To investigate this relationship, dynamic centrifuge model tests were conducted. The spacing between the grid-walls was 16 × 13m. The grid area was 208 m^2, corresponding to typical conditions in the residential areas of Urayasu. For such typical conditions, dynamic centrifuge model tests confirmed the settlement of a residential house (within 50 mm) [4]. The grid area of 208 m^2 corresponds to one house existing in one grid. Therefore, the adopted design policy is to construct one grid for one residential house.

3. Design Condition

For the design of grid-wall soil improvements for the Nakamachi area's 16 districts, the design conditions conforms to the MLIT Guidance [5] and consider the characteristics on Urayasu city.

3.1 Target of countermeasure

Table 1 shows the minimum requirement value for performance-based design of grid-wall soil improvements. The main target earthquake for the design is same the level as the main shock observed for 2011 Tohoku earthquake in Urayasu. A level 2 earthquake corresponds to a local earthquake. For the main target earthquake level, it is required that no obvious damage occurs for a residential house. To satisfy the above-mentioned performance, the requirement value must be either an *F*L that exceeds 1.0 in all liquefied layer or that both D_{cy} should be within 5 cm and H_1 should be exceed 5.0 m. D_{cy} indicates the index of settlement due to liquefaction based on the Recommendation for Design of Building Foundations [3]. There is no damage for residential house with a large enough value of H_1 [6]. For a level 2 earthquake, the requirement value is the stress level that occurs on the improved grid-wall. Namely, the shear stress of the grid-wall must not exceed the permissible value. The requirement value for a main target earthquake must be satisfied even after the occurrence of level 2 earthquake.

3.2 Earthquake waves in the design process

Figure 7 shows a wave of a main target earthquake that was observed at the seismic bedrock in engineering of Yumenoshima during the 2011 Tohoku earthquake. In design, the amplitude of the input motion to the seismic bedrock in engineering (V_s ≧ 400 m / s) is adjusted to the peak ground

Phot.3 Damage to a residential house in Urayasu due to liquefaction during the earthquake.

Tab. 1 Minimum requirement values for performance based-design of grid-wall soil improvements.

Design earthquake	Requirement performance	Performance guideline
Main target earthquake	Occurrence of no obvious damage due to liquefaction	①FL > 1.0 in all liquefied strata or ②Dcy ≦ 5 cm and H_1 ≦ 5 m
Level 2 earthquake	Maintain effectiveness of cuntermeasures	Occurred shear stress ≦ Permissible stress (improved soil)

Tab.2 Design seismic waves.

Design earthquake	Seismic wave	Magnitude, Maximum acceleration
Main target earthquake	Yumenoshima wave (observed in 2011.3.11)	Mw = 9.0、Max = 0.109g
Level 2 earthquake	Northern part of Tokyo Bay (simulated seismic wave)	Mw = 7.3、Max = 0.426g

acceleration as estimated from the peak ground acceleration during the 2011 Tohoku earthquake. The wave of a level 2 earthquake adopts a seismic wave recorded from the northern part of Tokyo Bay (Fig. 8). This earthquake wave is a simulated seismic wave of a local earthquake in Urayasu. The input motion amplitude at Nakamachi area's 16 districts has the same amplitude as shown in Fig. 8.

3.3 Soil parameters in design analysis

The design analysis was conducted using equivalent linear analysis, which requires the following soil parameters; the unit weight, shear wave velocity V_s, and the dynamic properties of the ground. The unit weight adopted the average value obtained at the first group consisting of five districts, where geological surveys were previously conducted. In design analysis, the dynamic properties of the ground for the liquefied stratum of F_s, A_{s1}, and A_{s2} were set up as shown in Fig. 9. The groundwater level of each district was set up with the observed groundwater level at the boring point. However, the groundwater level was 0.5 m below from the ground surface in the observed results, while the average groundwater level was almost 1.5 m below from the ground surface. In analysis, considering seasonal variations, the groundwater level was set up to be shallower. Therefore, the groundwater level was adopted as 1.0 m below from the ground surface for 10 of the 15 districts.

The thickness of the bank, called the B_s stratum was about 1.5 m. The liquefaction strength of the B_s stratum, which was obtained from Swedish weight sounding and cyclic tri-axial test, is large enough to mitigate from liquefaction during a main target earthquake. Therefore, the B_s stratum was regarded as non-liquefied stratum in the design. The F_c stratum was also regarded as a non-liquefied stratum due to the relationship between the plasticity index and the fine fraction content of soils obtained from laboratory tests. Assuming that the B_s stratum and the F_c stratum are regarded as non-liquefied stratums, H_1 from the ground surface exceeds 2.0 m in the major parts of 16 districts. The liquefaction strength of each district for the F_s stratum, the A_{s1} stratum, and

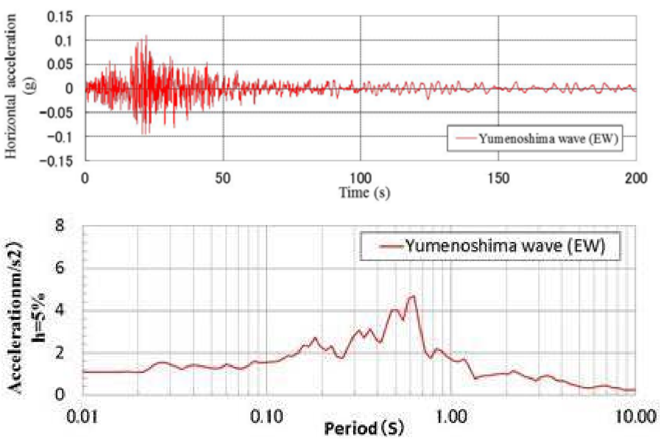

Fig.7 Seismic wave and acceleration response spectrum (main target earthquake).

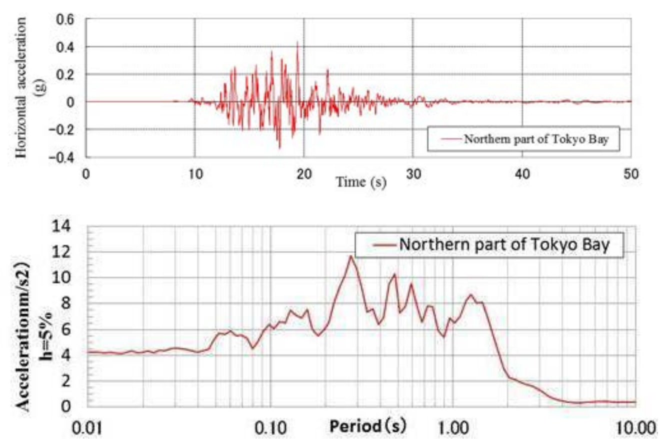

Fig.8 Seismic wave and acceleration response spectrum (level 2 earthquake)

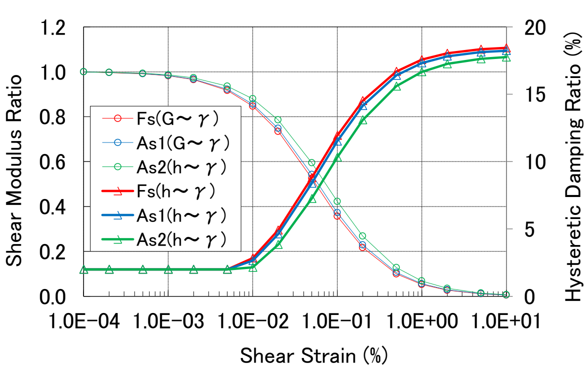

Fig.9 Dynamic properties G～γ, and h～γ (Fs, As1, and As2).

Tab.3 Liquefaction strength and liquefaction occurrence

District	Liquefaction strength (RL15)			Occurrence of liquefaction		
	Fs	As1	As2	Fs	As1	As2
A	0.171	0.210	0.279	×	×	○
B	0.147	0.182	0.256	×	×	○
C	0.162	0.248	0.241	×	○	○
D	0.167	0.169	0.360	×	×	○
E	0.162	0.276	0.239	×	○	△
F	0.178	0.203	0.241	×	△	○
G	0.217	0.251	0.282	×	△	○
H	0.199	0.190	0.319	×	—	○
I	0.201	—	0.253	×	—	△
J	0.209	0.172	0.267	×	×	○
K	0.148	0.190	0.375	×	×	○
L	0.184	0.230	0.259	×	×	○
M	0.180	0.174	0.486	×	×	○
N	0.215	0.175	0.259	×	×	○
O	0.184	0.181	0.286	×	×	○
P	0.148	0.187	0.478	×	×	○

× : Liquefaction　△ : Local liquefaction　○ : Non-liquefaction the A_{s2} stratum are shown in Tab. 4. The liquefaction strength was defined as a 3.75% shear strain with a single amplitude with 15 waves (*R*L15), and the liquefaction strength adopted in design was the average value. Table 3 also shows the judgment result for liquefaction which was obtained from one-dimensional equivalent linear analysis. The input motion to the seismic bedrock in engineering of each district was set up for a peak ground acceleration of the same level as the estimated one. Liquefaction occurs in the F_s stratum in all 16 districts. Liquefaction occurs in the As1 stratum in 4 of 16 districts. Liquefaction does not occur in the A_{s2} stratum in 14 districts, and partial liquefaction occurs in the A_{s2} stratum of 2 districts.

4. Verification of Numerical Method with Model Ground Conditions

The Urayasu committee adopted the soil profile to consider the countermeasures to mitigate liquefaction in 2012 (Fig. 10). The model ground condition was to refer to the stratum structure of the area where the most severe damage occurred due to liquefaction during the 2011 Tohoku earthquake. The stratum structure from the ground surface was B_s stratum filled with mountain sand, F_s stratum constructed with dredge soil, and A_{s1}・A_{s2} strata composed of natural deposits. Just below A_{s2}, loose A_c stratum was deposited 45 m below the ground level. The stratum structure of the 16 districts is similar to the model ground condition. Dynamic centrifuge model tests were conducted with the model ground conditions. According to the relationship between the grid area and the settlement of residential houses obtained from tests results, the analysis method for setting up the specifications of grid-wall soil improvements was verified.

4.1 Relationship between the grid area and the settlement of a residential house obtained from dynamic centrifuge model test results

Table 4 shows the liquefaction strength for the model's ground condition in Urayasu and from the experiments. In the experiments, the liquefied layer of the ground model was made using Toyoura sand and Urayasu sand. Urayasu sand was taken from erupted soil from Urayasu during the 2011 Tohoku earthquake. The liquefaction strength of the ground model in the experiment corresponded to the model's ground condition. The *D* value for

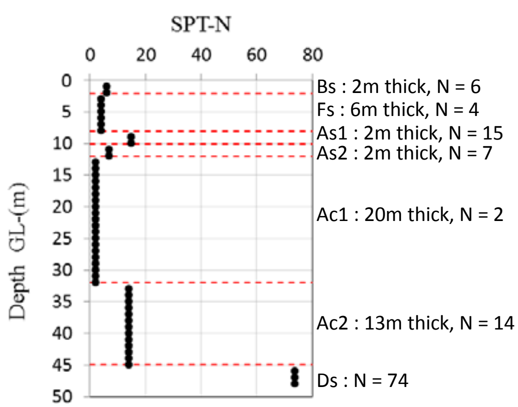

Fig.10 Ground model conditions.

Tab.4 Liquefaction strength (ground model and experiments)

Urayasu ground model			Experimental ground model			
Depth (m)	Layer	ε a = 2.5%, Stress ratio with 20 cycle times	Layer	ε a = 2.5%, Stress ratio with 20 cycle times	Layer	ε a = 2.5%, Stress ratio with 20 cycle times
0–2 m	Bs	0.25	Toyoura sand Dr = 50%	0.17	Urayasu sand D value= 90%	0.18
2–8 m	Fs	0.20				
8–10 m	As1	0.36	Toyoura sand Dr = 70%	0.22	Urayasu sand D value= 95%	0.28
10–12 m	As2	0.23				

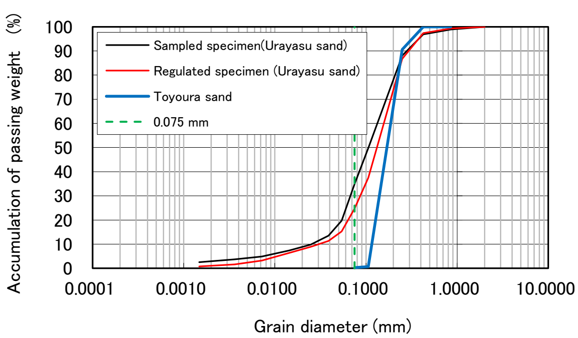

Fig.11 Grain size distribution for Urayasu and Toyoura sand.

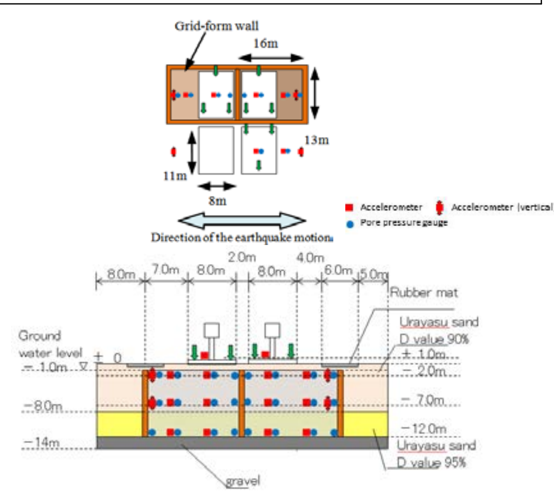

Fig.12 Plan view and cross-section for Case-6 (the cross-section is the countermeasure side).

controlling the density of Urayasu sand is defined as the ratio for the maximum dry density (ρ_{dmax} = 1.451 t/m^3). Toyoura sand was controlled using the relative density. Figure 11 shows the grain size distribution of Toyoura sand and Urayasu sand. The fine content of Urayasu sand was adjusted to 25%.

Figure 12 shows the plan view and cross section in Case-6 which countermeasures and the without mitigation measure were modeled. The measurements were converted to an actual scale from the models. The dynamic centrifuge model tests were conducted for 60 times gravity. The spacing of grid-walls was 16 and 13 m, which one house existed in each grid. The spacing between the grid-walls was defied as the distance from the center of the improved walls. The spacing between the residential house models was 2.0 m, and the center of the improved wall was at 1.0 m from the residential house model. The model liquefied layer was made with Urayasu sand. The grid-wall soil improvement model was made of acrylic, with a width of 0.9 m (Young's modulus E = 1.47×10^3 MPa). The Young's modulus E of acrylic corresponds to that of improved soil produced using the mechanical mixing method with a standard design strength f_c = 1.5 (N/mm^2). An Urayasu Wave was inputted at the base of the shaking box. The model of the residential house had two stories, and the flat dimensions were 8.0 m (direction of earthquake motion) and 11.0 m (orthogonal to the direction of the earthquake). The contact pressure of the model residential house was 8.4 (kN/m^2).

Figure 13 shows the relationship between the grid area and the settlement of the residential house. The grid area was defined with the surrounding area of the center of improved soil. The area of the 16 × 13 m grid was 208 m^2. The area of the 32 × 13 m grid was 416 m^2, and the area of the 32 × 26 m grid was 832 m^2. Since the grid area was small, the settlement of the residential house was minimal. Under the conditions of the 16 × 13 m grid, the average settlement of the residential houses was 50 mm, and it was about 40% compared with the without countermeasures. The average settlement of the residential house was almost the same for the case of Toyoura sand and for the case of Urayasu sand. In the case of a 20 × 20 m grid, which has an area of 400 m^2, the average settlement of the residential house was 71 mm. The grid area of the 20 × 20 m square grid was almost same as the 416 m^2 of the 32 × 13 m rectangular grid. Furthermore, the average settlement of the 32 × 13 m rectangular grid was 66 mm, which is similar to that of the square area's average settlement. This shows that it is reasonable to arrange the experimental results according to the grid area, and therefore the grid area was adopted as a design guideline.

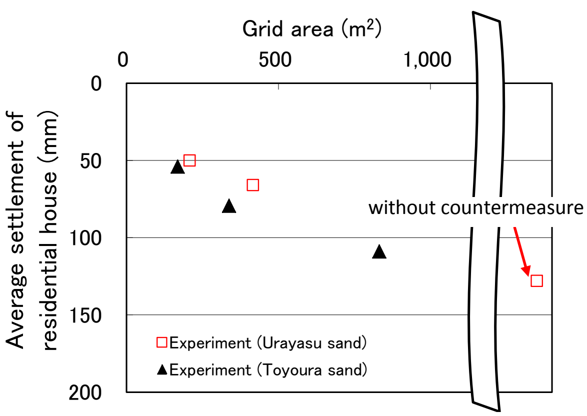

Fig.13 Relationship between the grid area and the settlement of the residential house in the experiments.

Tab.5 Soil parameters used in analysis.

Stratum	SPT-N value	Startum thickness (m)	Content rate of fine - grained fraction (%) Fc	Density (t/m^3) ρ	Shear wave velocity (m/s) Vs	Initial shear modulus (kPa) G_0	Poisson's ratio ν
Bs (dry)	6	1	18	1.80	145	38,038	0.49
Bs (saturated)	6	1	18	1.80	145	38,038	0.49
Fs	4	6	22	1.80	127	29,029	0.49
As1	15	2	21.9	1.80	197	70,067	0.49
As2	7	2	31	1.70	153	39,813	0.49
Ac1	2	20	93.6	1.50	133	26,534	0.49
Ac2	14	15	93.6	1.50	220	72,600	0.49
Ds (engineering base)	74	-	10	2.00	388	301,088	0.49

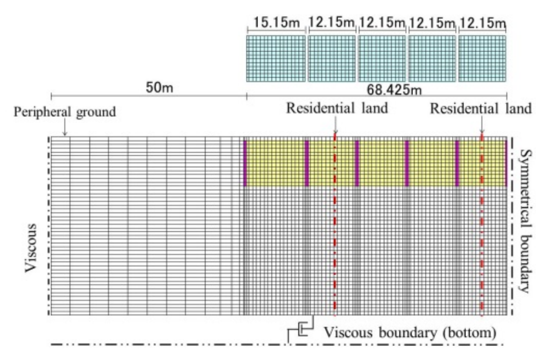

Fig.14 Quasi-three-dimensional model (1 grid for 1 residential land-area).

4.2 Analysis of the ground model

An analysis of the ground model (shown in Fig. 10) was conducted using equivalent linear analysis. Table 5 shows the soil parameters in the analysis. The grid-wall soil improvement was modeled using a quasi-three-dimensional model (Fig. 14). The quasi-three-dimensional model consisted of several two-dimensional sections. One section modeled the improved soil (orthogonal to the direction of the earthquake) and liquefied layer, and the other modeled the improved soil (direction of the earthquake motion). According to the boundary condition that the cross node of improved soil (orthogonal to the direction of the earthquake) and improved soil (direction of the earthquake motion) move in the same modes (Fig. 15), the three-dimensional shape of grid-wall soil improvement was modeled using a two-dimensional analysis model. The analysis was conducted for the without mitigation measures. The countermeasure analysis model changed the width *W* of the soil improvement (orthogonal to the direction of the earthquake) and the length *L* of the soil improvement (direction of the earthquake motion). *W* and *L* are defined in Fig. 15. The three analysis models for the countermeasures were one house within one grid (16 × 13 m grid), two houses within one grid (32 × 13 m grid), and four houses within one grid (32 × 26 m grid). In the analysis, the houses were not modeled.

Figure 16 shows the distribution of the maximum horizontal acceleration and *F*L in the depth direction with the without mitigation measures. The peak ground acceleration was 1.43 (m/s^2) for a Yumenoshima wave and 1.91 (m /s^2) for 1.4 times the amplitude of a Yumenoshima wave. For both amplitudes, *F*L was within 1.0 for all liquefied strata.

In the quasi-three-dimensional analysis, the shear stress occurring within the liquefied ground of the grid-wall soil improvement tend to underestimate values for cases with a high shear modulus of soil improvements. Figure 17 compares the settlement of the residential house in the experiments (shown in Fig. 13) and D_{cy} obtained from quasi-three-dimensional analysis using a 70 % shear modulus. The experimental results and analysis results exhibited good correspondence. In design using equivalent linear analysis with a quasi-three-dimensional model, the shear modulus of improved soil adopted the shear modulus reduced to 70%.

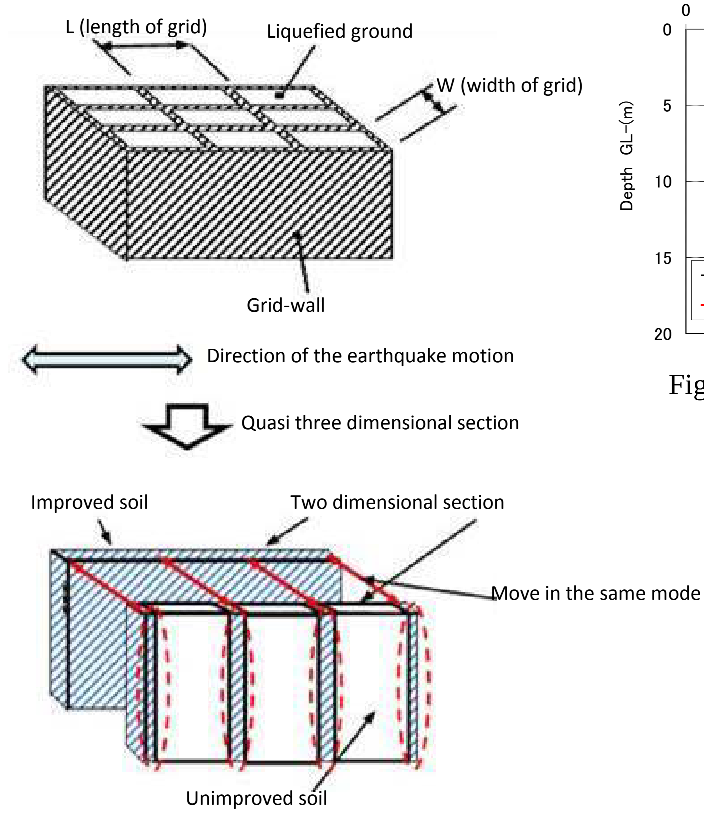

Fig.15 Method for producing a quasi-three -dimensional model.

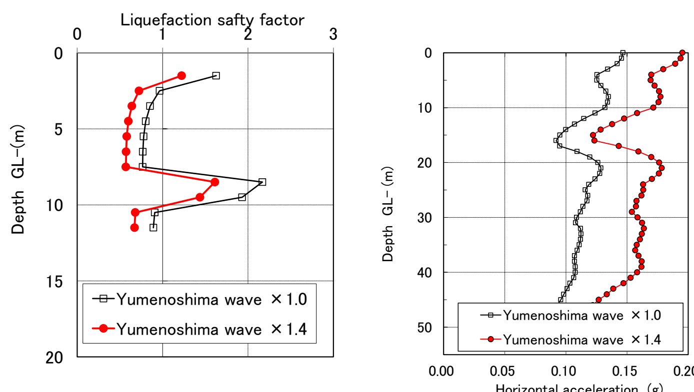

Fig.16 Response acceleration and liquefaction safety factor (without mitigation measures).

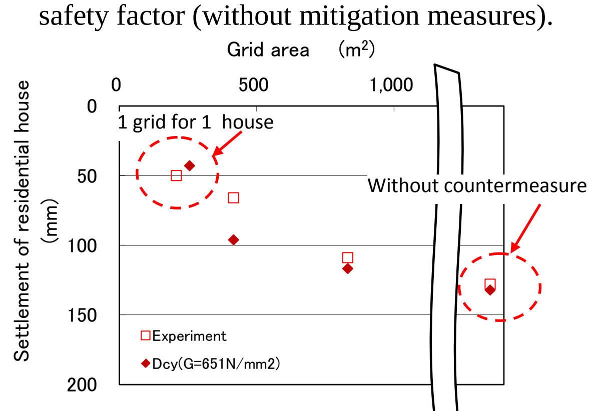

Fig.17 Comparison of the settlement of a residential house between Q3D and experiments.

5. Design of Grid-Wall Soil Improvements in C District

Using the analytical method mentioned in previous chapter, the design of grid-wall soil improvements was conducted for 4,103 residential houses in 16 districts. This chapter will describe the design process for C district, focusing on the selection process of the specifications for grid-wall soil improvements.

5.1 Site investigation

Figure 18 shows a plan view of C district. C district was composed of 98 houses in 7 blocks. The items for site investigation were classified as ‘residents’ and ‘roads’. For ‘resident’, the spacing of the neighboring houses was measured and obstacles to construction of grid-walls such as walls and plants were investigated. Then, the construction plan for ground improvement was prepared, including plans to remove and recover the obstacles. For ‘road’, obstacles such as buried sewage pipes were surveyed with as-built drawings. A construction plan for grid-wall soil improvements was also made while considering the possibility of removing buried sewage pipe. Figure 19 shows a construction plan view for grid-wall soil improvement. The mechanical mixing method was used for construction on ‘road’. A high pressure injection mixing method was used for the construction of narrow spaces in the spacing of houses and roads.

5.2 Geological surveys

Surveys with a standard penetration test (SPT) or a PDC [7] test were conducted with 50 to 100 m distances. The liquefaction strength in a liquefied stratum was calculated using the SPT-*N* value and the fine fraction content of soils was obtained from geological surveys. Figure 18 also shows the points of the geological surveys; the red circle shows the SPT test points, the blue rhomboids show the PDC test points. The categories of soil tests with the test specimens obtained from boreholes were physical characteristics, dynamic properties of ground, and cyclic tri-axial tests. PS logging test was conducted at one location. Following the geological survey results, the

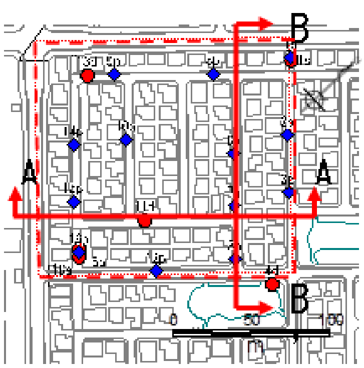

Fig.18 Plan view of C district

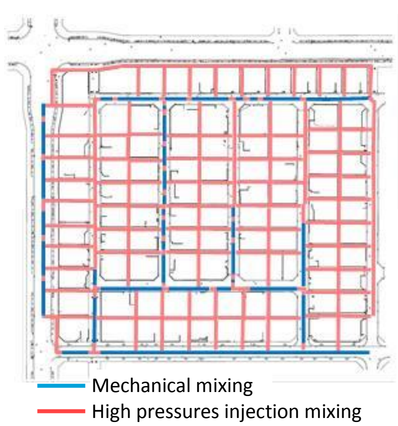

Fig.19 A plan view of the construction plan of grid-wall soil improvements.

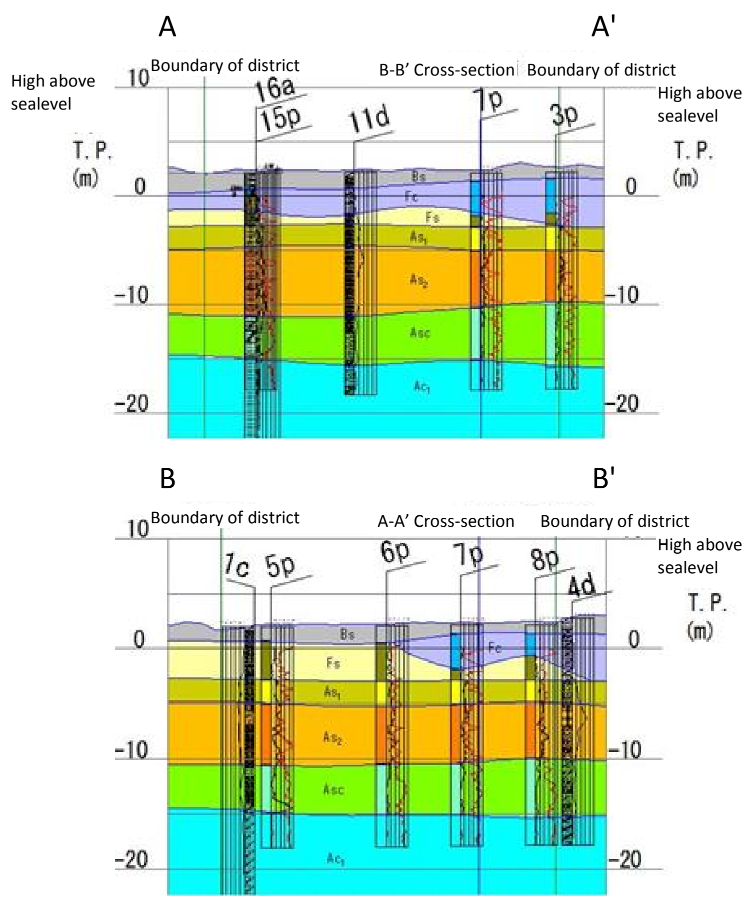

Fig.20 Geological cross-section in C district.

stratum layers were estimated. Figure 20 shows the geological sections, which were the A-A' section and the B-B' section drawn in the plan view (shown in Fig. 18). The design analysis was conducted for the above two geological sections. C district was located at the center of Nakamachi. From the ground surface, stratum layers were divided into bank (B_s stratum), landfill (F_s and F_c stratum) constructed with dredged soil until 5 to 6 m below ground level, and holocene sand (A_{s1}, A_{s2}, and A_{sc}) composed of natural deposits until 16 to 18 m below ground level (Fig. 20).

5.3 Design analysis for grid-wall soil improvements

For the cross-sections shown in Fig. 20, quasi-three-dimensional analysis models were produced (shown in Fig. 21). The bottom boundary condition used a viscous boundary. The side boundary condition used an energy transfer boundary. In the design analysis, one analysis model section was made with approximately 100 houses. Table 6 shows the soil parameters adopted in the design analysis. The effective width of the grid-wall was 0.85 m and the design strength of the improved soil wall was f_c=1.8 (N/mm^2). The initial shear modulus G_0 of improved soil was determined according to the Recommendation for Design of Ground Improvement for Building Foundations [8]. For the condition of f_c = 1.8 (N/mm^2), G_0 = 1114 (N/mm^2).

According to the comparison of results between quasi-three-dimensional analysis and the experiments, it was necessary to reduce the value of G_0 used in quasi-three-dimensional analysis by 70% from G_0=1114 (N/mm^2). Therefore, the value of G_0 used in the design analysis was 781 (N/mm^2). Figure 22 shows the dynamic properties of the improved soil according to reference documents. The dynamic properties of the ground adopted the same properties shown in Fig. 9.

The equivalent linear analysis gave a maximum value of shear stress τ_{max} at the center of liquefied ground within grid-walls, and FL was determined from a comparison of the equivalent shear stress ratio obtained with the

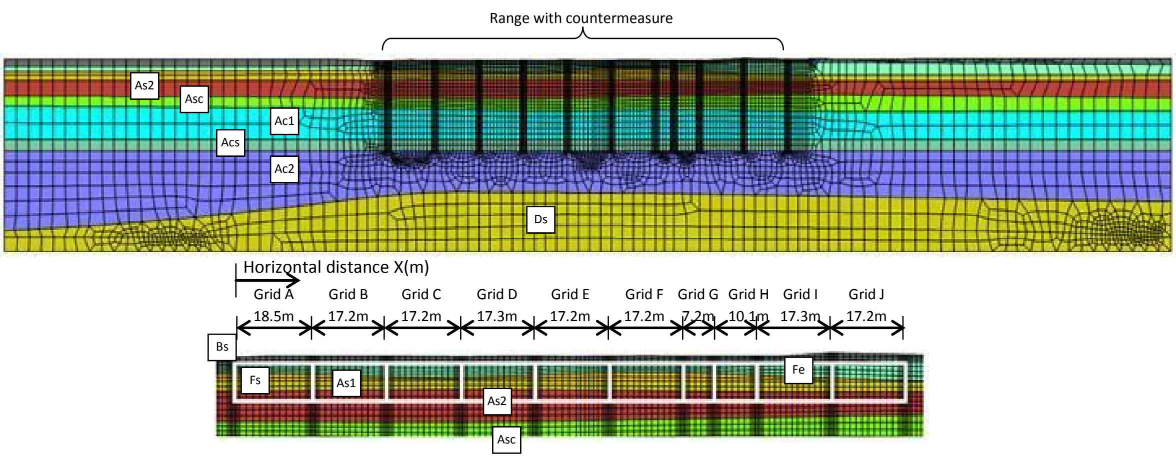

Fig.21 Quasi-three-dimensional analysis models used in design analysis (A-A' cross section).

Tab.6 Soil parameters used in design analysis for C district

Stratum	γ_t (kN/m^3)	γ' (kN/m^3)	ρ (kg/m^3)	Vs (m/s)	ν	G_0 (MN/m^2)
Bs	19.0	9.0	1.937	120	0.489	27.9
Fc	15.5	5.5	1.581	120	0.489	22.8
Fs	19.0	9.0	1.937	170	0.488	56.0
As1	19.0	9.0	1.937	170	0.488	56.0
As2	19.0	9.0	1.937	170	0.488	56.0
Asc	18.0	8.0	1.835	130	0.496	31.0
Ac1	16.0	6.0	1.632	130	0.496	27.6
Acs	16.5	6.5	1.683	150	0.495	37.9
Ac2(1)	16.0	6.0	1.632	150	0.491	36.7
Ac2(2)	16.0	6.0	1.632	200	0.491	65.3
Ds	18.5	8.5	1.886	310	0.480	181.3
Improved soil	20.0	10.0	2.041	-	0.260	781.0

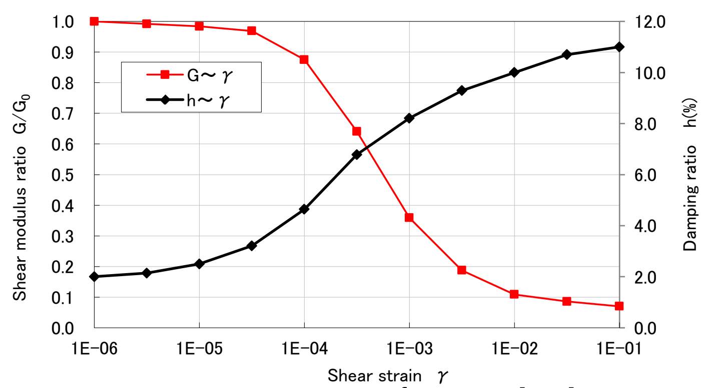

Fig.22 Dynamic properties of improved soil.

calculated τ_{max} and the liquefaction strength. The magnitude M_w of a main target earthquake was considered in the calculation of the shear stress occurring in liquefied ground. The correction coefficient γ_n was set as $\gamma_n = 0.1(M_w\text{-}1) = 0.8$. In the calculation of FL, the liquefaction strength adopted was the average value of the liquefaction strength obtained from the SPT test and the PDC test for the following strata; F_s, A_{s1}, and A_{s2}.

The grid area was distributed from 200 to 400 m^2. The relationship between the grid area and the settlement of a residential house shown in Fig. 13 was able to be applied for the design of C district due to the plan shape of the grid-form area in C district. Therefore, the width of quasi-three-dimensional model was set at various values, it is able to estimate the possibility of liquefaction and evaluation of the improved soil for a distributed wide area of a residential house. The depth of the gas pipe and water pipe buried from the road to the residential house was about 1 m below ground level. It is necessary to maintain sufficient spacing between pipes and the top of the grid-wall during construction. The high pressure injection mixing also requires a 1.5 m overburden from ground level. Therefore, the top of the grid-wall was set at 1.5 m below ground level. Since the bottom depth of the grid-wall was determined to satisfy the design guideline shown in Tab. 2, design analysis was conducted with the quasi-three-dimensional model where the bottom depths of the grid-form wall were 10, 11, and 12m below ground level.

Figure 23 shows the distribution of FL in the depth direction and the maximum value of the shear stress that occurred for improved soil. Under the condition where the bottom depth of the grid-wall was 10 m below ground level, against a main target earthquake, FL exceeded 1.0 for all depth of the liquefied layer. Furthermore, the shear stress for improved soil was within the design guidelines. The allowable stress τ_a of improved soil was adopted as 30% of f_c. A safety factor of 2/3 was adopted for a main target earthquake and 3/3 for a local earthquake. Following these conditions, τ_a was 360 kPa for a main target earthquake and 540 kPa for a local earthquake. The bottom depth of the grid-wall in C district was determined to satisfy the design guideline, i.e., a value of FL that exceeds 1.0 for all liquefied layers. The plan distribution of the bottom

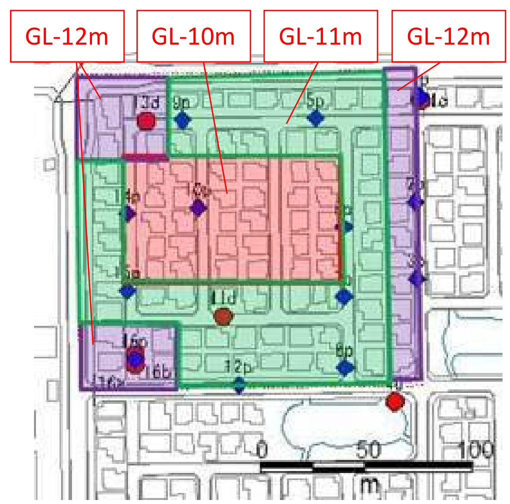

Fig.24 Plan view with bottom depth of grid-wall.

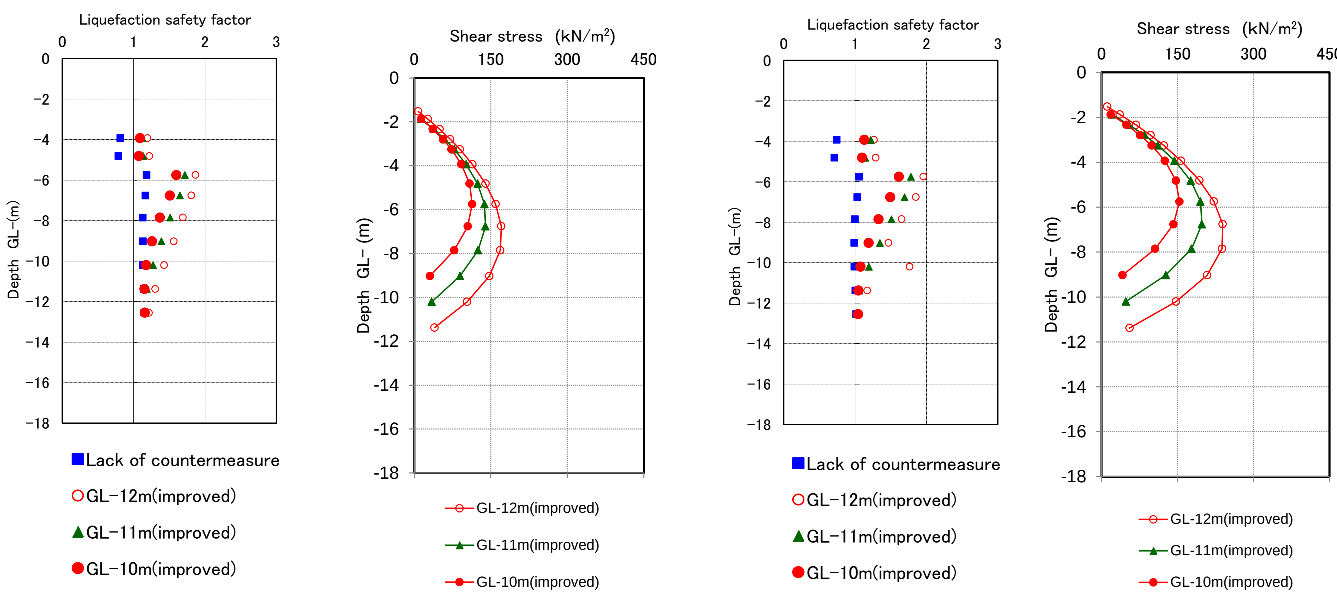

(a) Main target earthquake (b) Level 2 earthquake

Fig.23 Safety factor against Liquefaction and maximum shear stress distribution in the depth direction (A-A' cross section, grid-F).

depth of the grid- wall shown in Fig. 24 was determined to properly consider the analysis results and geological characteristics.

5. Conclusions

The damaged area in Urayasu was constructed using hydraulic dredging from 1965 to 1980. During the 2011 Tohoku earthquake, the occurrence of liquefaction in the F_s stratum and the A_s stratum was the main reason for damage to residential houses. In particular, occurrence of liquefaction in the F_s stratum was confirmed for a main target earthquake for every district in the design analysis. Conversely, occurrence of liquefaction in the A_{s1} stratum was only exhibited for four districts and the occurrence of liquefaction in the A_{s2} stratum was only observed for two districts. The design guidelines adopted the following two items: (1) During a main target earthquake at the same level as the 2011 earthquake, it is required that no obvious damage occurs for a residential house. (2) For a level 2 earthquake, the requirement value is not defined to mitigate liquefaction, but is set to the stress level that occurred for improved soil. Namely, the shear stress of a grid-wall must not exceed the permissible value. The requirement value for a main target earthquake must be satisfied even after the occurrence of a level 2 earthquake.

The performance, where no obvious occurrence damage is required for a residential house, was defined as a safety factor against liquefaction that exceeds 1.0 for all liquefied strata, or a H_1 value (thickness of the non-liquefied layer from ground level) that exceeds 5.0 m and a D_{cy} value (index of settlement due to liquefaction base on the Recommendation for Design of Building Foundations) that doesn't exceed 5 cm. This performance guideline was confirmed with analysis results obtained using equivalent linear analysis using a quasi-three-dimensional model. The verification of analytical results was conducted according to the equivalent linear simulation analysis using a quasi-three-dimensional model for dynamic centrifuge tests. For the various areas of residential houses, the effectiveness of the design method using various widths of quasi-three-dimensional analysis model was confirmed. The design guidelines adopted the grid area and did not adopt the spacing between the grid walls.

6. References

[1] Cooperative Research Reports of PWRI (1999): Design and Construction Manual of Countermeasures Against Liquefaction, Vol.186 (in Japanese).

[2] Uchida, A., Odajima, N. and Yamashita, K (2012): Performance of Piled Raft Foundation with Grid-Form Ground Improvement During the 2011 off the Pacific Coast of Tohoku Earthquake, Journal of Disaster Research, Vol.7, No.6, pp.726-732.

[3] Architectural Institute of Japan (2001): Recommendations for Design for Design of Building Foundations, pp.62 (in Japanese).

[4] Tsukuni, S., Uchida, A. and Konishi., K (2015): Effect of Grid-form Deep Mixing Walls to Prevent Liquefaction Damage of Small Houses, Proceedings of the 6th International Conference of Deep Mixing 2015, San Francisco.

[5] Ministry of Land, Infrastructure, Transport and Tourism Urban-Safety Affairs Division (2014): The city area liquefaction measures promotion guidance (in Japanese).

[6] Ishihara, K (1985): Stability of natural deposits during earthquake, Proc., 11th Int, Conf. on Soil Mechanics and Foundation Engineering, Vol. 1, pp.321-376.

[7] Sawada, S. (2009): Evaluation of differential settlement following liquefaction using. Piezo Drive Cone, 17th International Conference on Geotechnical Engineering, Alexandria, Egypt, 1064-1067.

[8] Architectural Institute of Japan (2006): Recommendations for Design of Ground Improvement for Building Foundations (in Japanese).